

# UC Irvine

## UC Irvine Previously Published Works

### Title

Flux growth and structure of two compounds with the  $EuIn_2P_2$  structure type,  $Aln_2P_2$  ( $A = Ca$  and  $Sr$ ), and a new structure type,  $Baln_2P_2$

### Permalink

<https://escholarship.org/uc/item/6sb0r7w1>

### Journal

Acta Crystallographica Section C: Structural Chemistry, 65(10)

### ISSN

0108-2701

### Authors

Rauscher, Japheth F  
Condron, Cathie L  
Beault, Tanya  
[et al.](#)

### Publication Date

2009-10-15

### DOI

10.1107/s0108270109035987

### Copyright Information

This work is made available under the terms of a Creative Commons Attribution License, available at <https://creativecommons.org/licenses/by/4.0/>

Peer reviewed

## Flux growth and structure of two compounds with the $\text{EuIn}_2\text{P}_2$ structure type, $\text{AIn}_2\text{P}_2$ ( $A = \text{Ca}$ and $\text{Sr}$ ), and a new structure type, $\text{BaIn}_2\text{P}_2$

Japheth F. Rauscher,<sup>a</sup> Cathie L. Condrón,<sup>a</sup> Tanya Beault,<sup>a</sup> Susan M. Kauzlarich,<sup>a\*</sup> Newell Jensen,<sup>b</sup> Peter Klavins,<sup>b</sup> Samuel MaQuilon,<sup>b</sup> Zachary Fisk<sup>b</sup> and Marilyn M. Olmstead<sup>a</sup>

<sup>a</sup>Department of Chemistry, University of California, One Shields Avenue, Davis, CA 95616, USA, and <sup>b</sup>Department of Physics, University of California, One Shields Avenue, Davis, CA 95616, USA

Correspondence e-mail: smkauzlarich@ucdavis.edu

Received 12 July 2009

Accepted 5 September 2009

Online 30 September 2009

Single crystals of the new Zintl phases  $\text{AIn}_2\text{P}_2$  [ $A = \text{Ca}$  (calcium indium phosphide),  $\text{Sr}$  (strontium indium phosphide) and  $\text{Ba}$  (barium indium phosphide)] have been synthesized from a reactive indium flux.  $\text{CaIn}_2\text{P}_2$  and  $\text{SrIn}_2\text{P}_2$  are isostructural with  $\text{EuIn}_2\text{P}_2$  and crystallize in the space group  $P6_3/mmc$ . The alkaline earth cations  $A$  are located at a site with  $\bar{3}m$  symmetry; In and P are located at sites with  $3m$  symmetry. The structure type consists of layers of  $A^{2+}$  cations separated by  $[\text{In}_2\text{P}_2]^{2-}$  anions that contain  $[\text{In}_2\text{P}_6]$  eclipsed ethane-like units that are further connected by shared P atoms. This yields a double layer of six-membered rings in which the In–In bonds are parallel to the  $c$  axis and to one another.  $\text{BaIn}_2\text{P}_2$  crystallizes in a new structure type in the space group  $P2_1/m$  with  $Z = 4$ , with all atoms residing on sites of mirror symmetry. The structure contains layers of  $\text{Ba}^{2+}$  cations separated by  $[\text{In}_2\text{P}_2]^{2-}$  layers of staggered  $[\text{In}_2\text{P}_6]$  units that form a mixture of four-, five- and six-membered rings. As a consequence of this more complicated layered structure, both the steric and electronic requirements of the large  $\text{Ba}^{2+}$  cation are met.

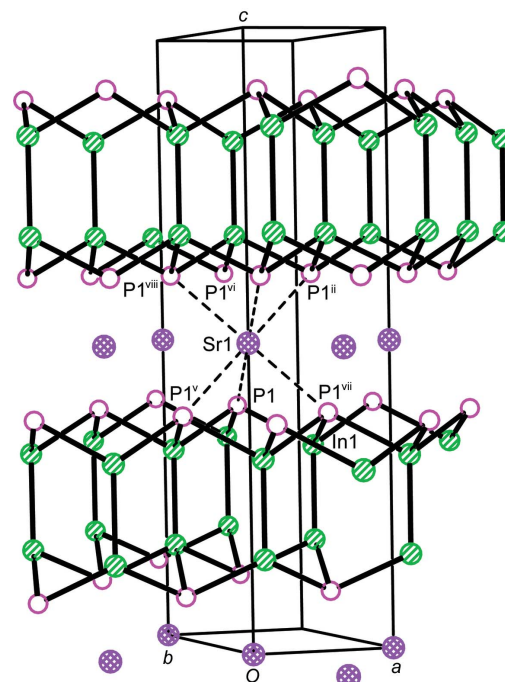
### Comment

Layered ternary compounds,  $\text{AB}_2\text{X}_2$  ( $A =$  rare earth or alkaline earth metal;  $B =$  main group, metalloid;  $X =$  main group 14–17 element) or 1–2–2 phases, favor the  $\text{ThCr}_2\text{Si}_2$  ( $I4/mmm$ ) structure type, with the  $\text{CaAl}_2\text{Si}_2$  structure type ( $P\bar{3}m1$ ) as a distant second (Grytsiv *et al.*, 2002; Hellmann *et al.*, 2007). There are a few other less commonly observed structure types for layered main group metalloids, such as  $\alpha\text{-BaCu}_2\text{S}_2$  ( $Pnma$ ; Leoni *et al.*, 2003) observed for  $\text{BaAl}_2\text{Si}_2$  (Condrón *et al.*, 2007), and  $\text{EuIn}_2\text{P}_2$  (Jiang & Kauzlarich, 2006). In addition to

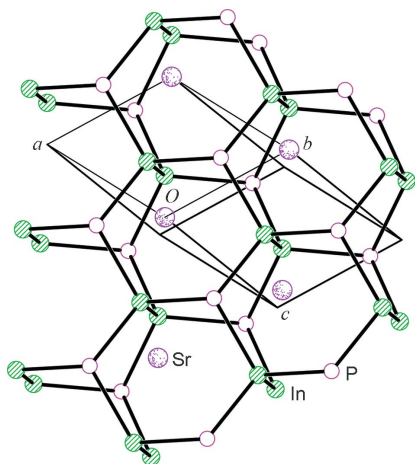
layered structure types, there is at least one example of a 1–2–2 phase with a three-dimensional structure, as found in  $\text{BaGa}_2\text{Sb}_2$  (Kim & Kanatzidis, 2001). More complex two- and three-dimensional structures composed of alkaline earth, In and P have also been reported, such as  $\text{Ba}_2\text{In}_5\text{P}_5$  (Mathieu *et al.*, 2008),  $\text{Ba}_{14}\text{InP}_{11}$  (Carrillo-Cabrera *et al.*, 1996) and  $\text{Ba}_3\text{In}_2\text{P}_4$  (Sommer *et al.*, 1998).

The rare earth Zintl phase  $\text{EuIn}_2\text{P}_2$  contains two-dimensional layers of  $\text{Eu}^{2+}$  cations dispersed between layers of  $[\text{In}_2\text{P}_2]^{2-}$  anions.  $\text{EuIn}_2\text{P}_2$  has been shown to exhibit colossal magnetoresistance (Jiang & Kauzlarich, 2006). The temperature-dependent magnetoresistance and the magneto-optical behavior of this compound suggest interaction between conduction electrons and local spins (Jiang & Kauzlarich, 2006; Pfuner *et al.*, 2008). The alkaline earth analogs of  $\text{EuIn}_2\text{P}_2$  were prepared in order to provide a nonmagnetic analog for heat capacity and electrical transport studies. The existence of the Sr analog has been alluded to in a recent publication (Mathieu *et al.*, 2008), although the structural details were not provided. Here, two new members of the  $P6_3/mmc$  structure type are presented, along with one new structure type,  $P2_1/m$ . Both structures can be described as composed of  $\text{In}_2\text{P}_6$  ethane-like moieties (either eclipsed or staggered) connected through the P atoms in such a fashion as to form layers separated by alkaline earth cations.

$\text{CaIn}_2\text{P}_2$  and  $\text{SrIn}_2\text{P}_2$  are isostructural in the space group  $P6_3/mmc$ . A view of  $\text{SrIn}_2\text{P}_2$  emphasizing the layered structure is provided in Fig. 1.  $\text{AIn}_2\text{P}_2$  ( $A = \text{Ca}$  and  $\text{Sr}$ ) contains alter-



**Figure 1**  
The crystal structure of  $\text{SrIn}_2\text{P}_2$ , viewed down the  $[110]$  direction, showing the  $[\text{In}_2\text{P}_2]^{2-}$  layers and the trigonal antiprismatic coordination of Sr. Atoms are shown at an arbitrary size. [Symmetry codes: (v)  $x - 1, y - 1, z$ ; (ii)  $-x + 1, -y + 1, -z + 1$ ; (vi)  $-x, -y, -z + 1$ ; (vii)  $x, y - 1, z$ ; (viii)  $-x, -y + 1, -z + 1$ .]

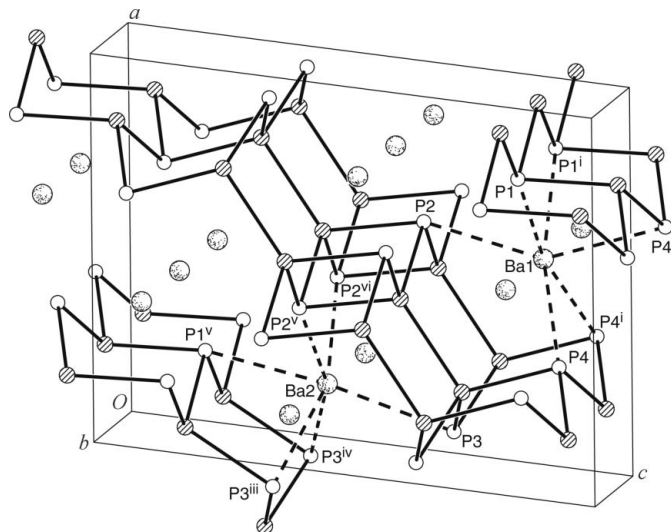

**Figure 2**

A view approximately perpendicular to the InP layer of  $\text{SrIn}_2\text{P}_2$ , showing the presence of six-membered rings and eclipsed  $\text{P}_3\text{InInP}_3$  units. The  $\text{Sr}^{2+}$  cations are symmetrically placed above the six-membered rings but are shown offset for clarity.

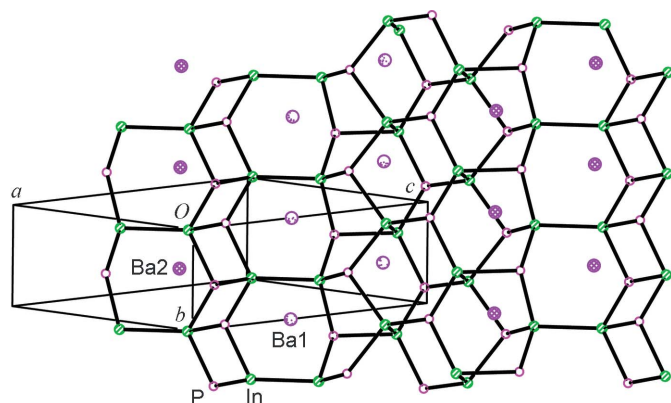
nating layers of  $[\text{In}_2\text{P}_2]^{2-}$  that are parallel to (001) and charge balanced by  $A^{2+}$  cationic layers stacked along the  $c$  axis. The alkaline earth element resides on Wyckoff position  $a$  (multiplicity 2) with  $\bar{3}m$  site symmetry. As shown in Fig. 1, its coordination environment consists of six P atoms in a trigonal antiprismatic arrangement. The In cation resides on Wyckoff position  $f$  (multiplicity 4) with  $3m$  symmetry. There are three surrounding P atoms in a pyramidal arrangement and an apical In cation. The centroid of the In–In bond is a site of  $\bar{6}m2$  ( $D_{3h}$ ) symmetry; thus, the ethane-related  $\text{P}_3\text{In}–\text{InP}_3$  unit has eclipsed P atoms. Each P atom [also at Wyckoff position  $f$  (multiplicity 4) with  $3m$  symmetry] has three equal bonds to In, as well as three equal bonds to Ca (Sr). The  $\text{P}_3\text{In}–\text{InP}_3$  units are connected in parallel *via* bridging P atoms to form a double layer of six-membered rings. The Ca or Sr cations are centered above each ring and form layers above and below each double layer of rings, as shown in Fig. 2.

The In–P bonds are considered to be covalent, whereas the In–Ca (Sr) interactions are electrostatic in origin. By Zintl electron counting (Kauzlarich, 1996), each P atom has a lone pair. The lone pair may have largely an  $s$  character, since its simultaneous interaction with three Sr atoms (Ca atoms) shows it to be nondirectional. The majority of the bond distances increase from the Ca to the Sr compound, as expected; the In–In<sup>i</sup> [symmetry code: (i)  $x, y, -z + \frac{1}{2}$ ] distances are equal within experimental error for both compounds. The previously reported Eu phase contains intermediate distances (Jiang & Kauzlarich, 2006).

$\text{BaIn}_2\text{P}_2$  adopts a new structure type with greater complexity and geometric distortion in the space group  $P2_1/m$ . Each atom resides on a crystallographic mirror plane. The structure is similar to  $\text{CaIn}_2\text{P}_2$  and  $\text{SrIn}_2\text{P}_2$  in that it contains alternating layers of  $[\text{In}_2\text{P}_2]^{2-}$  sheets, parallel to the (101) plane, that are charge balanced by  $A^{2+}$  cationic layers, as shown in Fig. 3. The In–In distances of 2.7625 (19) and 2.7620 (13) Å, corresponding to  $\text{CaIn}_2\text{P}_2$  and  $\text{SrIn}_2\text{P}_2$ ,


**Figure 3**

The crystal structure of  $\text{BaIn}_2\text{P}_2$ , viewed down the  $b$  axis. For clarity, Ba atoms are shown as dotted circles, P atoms as open circles and In atoms as shaded bottom left to upper right circles. Dashed lines show the six-coordinate environment for Ba1 and Ba2. [Symmetry codes: (i)  $x, y - 1, z$ ; (ii)  $-x + 1, -y + 1, -z + 2$ ; (iii)  $-x, -y + 1, -z + 1$ ; (iv)  $-x, -y + 1, -z + 1$ ; (v)  $-x + 1, -y + 1, -z + 1$ ; (vi)  $-x + 1, -y, -z + 1$ .]


**Figure 4**

A view approximately perpendicular to the InP layer of  $\text{BaIn}_2\text{P}_2$ . The positioning of  $\text{Ba}^{2+}$  cations above the four-, five- and six-membered rings is shown. In order to distinguish between Ba1 and Ba2, Ba1 cations are shown with dotted circles and Ba2 cations are shown with cross-hatched circles.

respectively, are bracketed by the two In–In bond distances of 2.7460 (10) [In2–In3<sup>vi</sup>; symmetry code: (vi)  $2 - x, -y, 2 - z$ ] and 2.8161 (10) Å (In1–In4) observed in  $\text{BaIn}_2\text{P}_2$ . There are two crystallographic sites for Ba cations in this structure. Each Ba is coordinated by six P atoms in a distorted trigonal antiprismatic arrangement, as shown in Fig. 3. The In coordination in  $\text{BaIn}_2\text{P}_2$  is similar to that in  $\text{CaIn}_2\text{P}_2$  and  $\text{SrIn}_2\text{P}_2$  in that it is comprised of another In cation and three P atoms, forming a  $\text{P}_3\text{In}–\text{InP}_3$  unit. However, in this structure, the ethane-like moiety is staggered and has noncrystallographic  $D_{3d}$  symmetry. The  $[\text{In}_2\text{P}_2]^{2-}$  layers are markedly different in  $\text{BaIn}_2\text{P}_2$  and consist of four-, five- and six-membered rings. A

view roughly perpendicular to the InP layer (Fig. 4) emphasizes this difference when compared with Fig. 2. The lower symmetry in the layer in  $\text{BaIn}_2\text{P}_2$  is likely related to the necessity to accommodate the larger  $\text{Ba}^{2+}$  cation (Shannon, 1976). If one assumes that the separation between cations is linked to the repeat distances of the six-membered  $(\text{InP})_3$  rings [4.0220 (17) Å in  $\text{CaIn}_2\text{P}_2$  and 4.0945 (16) Å in  $\text{SrIn}_2\text{P}_2$ ], it is apparent that the  $\text{EuIn}_2\text{P}_2$  structure type cannot accommodate Ba. In  $\text{BaIn}_2\text{P}_2$ , the shortest  $\text{Ba}\cdots\text{Ba}$  distance is 4.1789 (3) Å.

There are many examples where the identity of the cation provides different structures for isoelectronic series of compounds and this is also the case for Zintl and intermetallic phases (Kauzlarich, 1996; Nesper, 1990). For example,  $\text{AMn}_2\text{P}_2$  ( $A = \text{Sr}$  and  $\text{Ba}$ ) assumes different structure types depending on the identity of the cation:  $\text{SrMn}_2\text{P}_2$  crystallizes in the  $\text{CaAl}_2\text{Si}_2$  structure type, whereas  $\text{BaMn}_2\text{P}_2$  crystallizes in the  $\text{ThCr}_2\text{Si}_2$  structure type (Brock *et al.*, 1994). This was attributed to the difference in cation coordination: octahedral for the cation site in  $\text{CaAl}_2\text{Si}_2$  versus cubic in the  $\text{ThCr}_2\text{Si}_2$  structure type. Electronic considerations have been shown to play an important role in dictating structure and properties for other isoelectronic series (Alemany *et al.*, 2008; Xia & Bobev, 2007, 2008; Kim *et al.*, 2008). For  $\text{AIn}_2\text{P}_2$  ( $A = \text{Ca}$  and  $\text{Sr}$ ), the  $\text{EuIn}_2\text{P}_2$  structure type, the six-membered ring structure of the nonmetal layer cannot accommodate the size of the Ba cation and a new structure type is adopted.

Of the published structures of the combination of alkaline earth cation and group 13 and 15 elements,  $\text{Ba}_2\text{In}_5\text{P}_5$  is a recent example of a layered structure that is built up from ethane-like moieties (Mathieu *et al.*, 2008). The bond distances and angles in this compound are very similar to those observed in  $\text{BaIn}_2\text{P}_2$  presented herein. The structure of  $\text{Ba}_2\text{In}_5\text{P}_5$  can be described as containing two staggered ethane-like moieties similar to that observed in the  $\text{BaIn}_2\text{P}_2$  structure type, with the In—In bonds arranged parallel to each other and connected *via* P atoms. However, in  $\text{Ba}_2\text{In}_5\text{P}_5$ , two of the parallel moieties are joined through a P atom by a highly distorted  $\text{InP}_4$  tetrahedron.

The ethane-like moiety is also observed in the three-dimensional framework structures of  $\text{BaGa}_2\text{Sb}_2$  (Kim & Kanatzidis, 2001) and  $\text{Ba}_3\text{Ga}_4\text{Sb}_5$  (Park *et al.*, 2003). Both  $\text{BaGa}_2\text{Sb}_2$  and  $\text{Ba}_3\text{Ga}_4\text{Sb}_5$  adopt unique structure types that contain tunnels wherein the  $\text{Ba}^{2+}$  cations reside (Kim & Kanatzidis, 2001; Park *et al.*, 2003).

$\text{AIn}_2\text{P}_2$  ( $A = \text{Ca}$ ,  $\text{Sr}$  and  $\text{Ba}$ ) can be considered Zintl phases where there is electrostatic bonding between the alkaline earth cation and the layered anion (Kauzlarich, 1996). The basic building block of the ethane-like moiety is a common element in compounds composed of alkaline earth, group 13 and group 15 elements. Similar to the molecule ethane, this moiety can have a staggered or eclipsed conformation, however, it has a strong preference for a staggered conformation. This moiety is connected through shared P atoms to form extended structures in these compounds. The interaction of the P atoms with the cation, rather than the In—In bond length, may determine whether the moiety is eclipsed or

staggered, as the In—In bond is both the shortest and longest in the  $\text{BaIn}_2\text{P}_2$  compound (moiety is staggered) compared with the Ca (Sr) compounds (moiety is eclipsed).

## Experimental

$\text{AIn}_2\text{P}_2$  crystals were grown by reaction of the pure elements in an alumina crucible with an  $A:\text{In}:\text{P}$  molar ratio of 3:110:6, where  $A = \text{Ca}$ ,  $\text{Sr}$  or  $\text{Ba}$ . The metals, *viz.* Ca (Aldrich, 99.99% purity), Sr (Aldrich, 99% purity), Ba (Aldrich, 99% purity) and In (Cerac, 99.99% purity), were cut into small pieces and layered in a 5 ml crucible with indium on the top and bottom, and sealed under vacuum in quartz tubes. All materials were handled under an inert atmosphere or under vacuum. The reaction contents were heated in a programmable furnace at a rate of 60 K  $\text{h}^{-1}$  to 1373 K, maintained at that temperature for 16 h, cooled at a rate of 2 K  $\text{h}^{-1}$  to 1146 K, maintained at that temperature for 24 h and centrifuged to remove molten In flux. The crystals were then removed after breaking the quartz jacket in air. In the cases of Ca and Sr, the reactions yielded a few highly reflective black plate-like crystals on the sides and bottom of the crucible. In the Ba reactions, larger yields of black needle-shaped crystals were found within the crucible. All the crystals were found to be air stable. Attempts were made to increase the yield by decreasing the flux ratio, but this had the opposite effect of lowering the yield. In the case of Ba, some crystals of  $\text{Ba}_2\text{In}_5\text{P}_5$  (Mathieu *et al.*, 2008) were also present. The  $\text{Ba}_2\text{In}_5\text{P}_5$  phase is reported to be air sensitive and decomposed upon exposure to air, whereas the  $\text{BaIn}_2\text{P}_2$  crystals remained stable in air. The best formed crystals and highest yields of the 1–2–2 phases were for Ba.

The chemical composition of the Ba crystals was verified with an SEM (scanning electron microscopy) microprobe on a single crystal using a Camera SX-100 Electron Probe Microanalyzer equipped with a wavelength-dispersive spectrometer and calibrated standards. The samples were prepared by embedding the crystals in epoxy and polishing to ensure smooth surfaces. Each sample was scanned with a spot size of 1  $\mu\text{m}$  and data were collected at five to eight points along its surface. Composition totals for all points summed to 100%. The compositions were calculated as the average of the five points and provided the composition  $\text{Ba}_{1.00(4)}\text{In}_{2.023(6)}\text{P}_{2.020(3)}$ , in good agreement with the refined structure.

## $\text{CaIn}_2\text{P}_2$

### Crystal data

$\text{CaIn}_2\text{P}_2$	$Z = 2$
$M_r = 331.66$	Mo $K\alpha$ radiation
Hexagonal, $P6_3/mmc$	$\mu = 10.97 \text{ mm}^{-1}$
$a = 4.0220$ (17) Å	$T = 90 \text{ K}$
$c = 17.408$ (8) Å	$0.42 \times 0.40 \times 0.12 \text{ mm}$
$V = 243.87$ (18) Å <sup>3</sup>	

### Data collection

Bruker SMART 1000 diffractometer	3448 measured reflections
Absorption correction: multi-scan (SADABS; Sheldrick, 2003)	179 independent reflections
$T_{\min} = 0.021$ , $T_{\max} = 0.268$	153 reflections with $I > 2\sigma(I)$
	$R_{\text{int}} = 0.055$

### Refinement

$R[F^2 > 2\sigma(F^2)] = 0.028$	10 parameters
$wR(F^2) = 0.073$	$\Delta\rho_{\max} = 1.14 \text{ e \AA}^{-3}$
$S = 1.27$	$\Delta\rho_{\min} = -2.15 \text{ e \AA}^{-3}$
179 reflections	

**Table 1**

 Selected geometric parameters (Å, °) for  $\text{CaIn}_2\text{P}_2$ .

Ca1—P1	2.936 (2)	In1—In1 <sup>i</sup>	2.7625 (19)
In1—P1	2.6021 (16)		
P1—Ca1—P1 <sup>ii</sup>	93.54 (7)	P1—In1—In1 <sup>i</sup>	116.82 (6)
P1 <sup>iii</sup> —In1—P1	101.22 (7)	In1 <sup>iv</sup> —P1—In1	101.22 (7)

 Symmetry codes: (i)  $x, y, -z + \frac{1}{2}$ ; (ii)  $-x + 1, -y + 1, -z + 1$ ; (iii)  $x + 1, y, z$ ; (iv)  $x, y + 1, z$ .

## $\text{SrIn}_2\text{P}_2$

### Crystal data

$\text{SrIn}_2\text{P}_2$	$Z = 2$
$M_r = 379.20$	Mo $K\alpha$ radiation
Hexagonal, $P6_3/mmc$	$\mu = 19.55 \text{ mm}^{-1}$
$a = 4.0945 (16) \text{ \AA}$	$T = 90 \text{ K}$
$c = 17.812 (7) \text{ \AA}$	$0.34 \times 0.24 \times 0.19 \text{ mm}$
$V = 258.61 (18) \text{ \AA}^3$	

### Data collection

Bruker SMART 1000 diffractometer	3694 measured reflections
Absorption correction: multi-scan (SADABS; Sheldrick, 2003)	189 independent reflections
$T_{\min} = 0.014, T_{\max} = 0.057$	168 reflections with $I > 2\sigma(I)$
	$R_{\text{int}} = 0.035$

### Refinement

$R[F^2 > 2\sigma(F^2)] = 0.015$	10 parameters
$wR(F^2) = 0.037$	$\Delta\rho_{\text{max}} = 0.60 \text{ e \AA}^{-3}$
$S = 1.25$	$\Delta\rho_{\text{min}} = -0.78 \text{ e \AA}^{-3}$
189 reflections	

## $\text{BaIn}_2\text{P}_2$

### Crystal data

$\text{BaIn}_2\text{P}_2$	$V = 538.34 (7) \text{ \AA}^3$
$M_r = 428.92$	$Z = 4$
Monoclinic, $P2_1/m$	Mo $K\alpha$ radiation
$a = 9.9652 (8) \text{ \AA}$	$\mu = 16.15 \text{ mm}^{-1}$
$b = 4.1789 (3) \text{ \AA}$	$T = 90 \text{ K}$
$c = 12.9834 (10) \text{ \AA}$	$0.23 \times 0.15 \times 0.09 \text{ mm}$
$\beta = 95.326 (2)^\circ$	

### Data collection

Bruker SMART 1000 diffractometer	7899 measured reflections
Absorption correction: multi-scan (SADABS; Sheldrick, 2003)	1753 independent reflections
$T_{\min} = 0.119, T_{\max} = 0.324$	1452 reflections with $I > 2\sigma(I)$
	$R_{\text{int}} = 0.037$

### Refinement

$R[F^2 > 2\sigma(F^2)] = 0.038$	62 parameters
$wR(F^2) = 0.093$	$\Delta\rho_{\text{max}} = 2.56 \text{ e \AA}^{-3}$
$S = 1.03$	$\Delta\rho_{\text{min}} = -2.48 \text{ e \AA}^{-3}$
1753 reflections	

There are a number of residual peaks in the final difference map of  $\text{BaIn}_2\text{P}_2$  that do not appear to be due to twinning or disorder, but may arise from inadequate absorption correction or from stacking faults.

For all compounds, data collection: *SMART* (Bruker, 2003); cell refinement: *SAINTE* (Bruker, 2003); data reduction: *SAINTE*; program(s) used to solve structure: *SHELXS97* (Sheldrick, 2008); program(s) used to refine structure: *SHELXL97* (Sheldrick, 2008);

**Table 2**

 Selected geometric parameters (Å, °) for  $\text{SrIn}_2\text{P}_2$ .

Sr1—P1	3.0572 (12)	In1—In1 <sup>i</sup>	2.7620 (13)
In1—P1	2.6216 (11)		
P1—Sr1—P1 <sup>ii</sup>	95.92 (4)	P1—In1—In1 <sup>i</sup>	115.62 (3)
P1 <sup>iii</sup> —In1—P1	102.69 (4)	In1 <sup>iv</sup> —P1—In1	102.69 (4)

 Symmetry codes: (i)  $x, y, -z + \frac{1}{2}$ ; (ii)  $-x + 1, -y + 1, -z + 1$ ; (iii)  $x + 1, y, z$ ; (iv)  $x, y + 1, z$ .

**Table 3**

 Selected bond lengths (Å) for  $\text{BaIn}_2\text{P}_2$ .

Ba1—P1	3.218 (2)	In1—P2	2.6283 (17)
Ba1—P2	3.206 (3)	In1—In4	2.8161 (10)
Ba1—P4	3.267 (2)	In2—P1	2.6122 (17)
Ba1—P4 <sup>i</sup>	3.290 (3)	In2—P3 <sup>v</sup>	2.673 (3)
Ba2—P1 <sup>iv</sup>	3.233 (3)	In2—In3 <sup>vi</sup>	2.7460 (10)
Ba2—P2 <sup>ii</sup>	3.139 (2)	In3—P1	2.587 (3)
Ba2—P3 <sup>iii</sup>	3.227 (2)	In3—P4 <sup>vii</sup>	2.6350 (17)
Ba2—P3	3.438 (3)	In4—P3	2.6296 (18)
In1—P2 <sup>ii</sup>	2.624 (3)	In4—P4	2.612 (3)

 Symmetry codes: (i)  $-x + 1, -y, -z + 2$ ; (ii)  $-x + 1, -y, -z + 1$ ; (iii)  $-x, -y - 2, -z + 1$ ; (iv)  $-x + 1, -y - 1, -z + 1$ ; (v)  $x + 1, y + 1, z$ ; (vi)  $-x + 2, -y, -z + 2$ ; (vii)  $-x + 1, -y - 1, -z + 2$ .

molecular graphics: *SHELXTL* (Sheldrick, 2008); software used to prepare material for publication: *SHELXL97*.

This work was supported by the National Science Foundation (grant Nos. DMR-0600742 and DMR-0433560). CLC acknowledges a Tyco Electronics Foundation Fellowship in functional materials. The Bruker SMART 1000 diffractometer was funded in part by NSF Instrumentation grant No. CHE-9808259.

Supplementary data for this paper are available from the IUCr electronic archives (Reference: FA3198). Services for accessing these data are described at the back of the journal.

## References

- Aleman, P., Llunell, M. & Canadell, E. (2008). *J. Comput. Chem.* **29**, 2144–2153.
- Brock, S. L., Greedan, J. E. & Kauzlarich, S. M. (1994). *J. Solid State Chem.* **109**, 416–418.
- Bruker (2003). *SMART* and *SAINTE*. Bruker AXS Inc., Madison, Wisconsin, USA.
- Carrillo-Cabrera, W., Somer, M., Peters, K. & von Schnering, H. G. (1996). *Chem. Ber.* **129**, 1015–1023.
- Condron, C. L., Hope, H., Piccoli, P. M. B., Schultz, A. J. & Kauzlarich, S. M. (2007). *Inorg. Chem.* **46**, 4523–4529.
- Grytsiv, A., Kaczorowski, D., Leithe-Jasper, A., Rogl, P., Godart, C., Potel, M. & Noël, H. (2002). *J. Solid State Chem.* **163**, 37–43.
- Hellmann, A., Lohken, A., Wurth, A. & Mewis, A. (2007). *Z. Naturforsch. Teil B*, **62**, 155–161.
- Jiang, J. & Kauzlarich, S. M. (2006). *Chem. Mater.* **18**, 435–441.
- Kauzlarich, S. M. (1996). *Chemistry, Structure, and Bonding of Zintl Phases and Ions*, edited by S. M. Kauzlarich, pp. 245–274. New York: VCH Publishers.
- Kim, S.-J. & Kanatzidis, M. G. (2001). *Inorg. Chem.* **40**, 3781–3785.
- Kim, S. J., Ponou, S. & Fassler, T. F. (2008). *Inorg. Chem.* **47**, 3594–3602.
- Leoni, S., Carrillo-Cabrera, W., Schnelle, W. & Grin, Y. (2003). *Springer Ser. Solid State Sci.* **5**, 139–148.
- Mathieu, J., Achey, R., Park, J.-H., Purcell, K. M., Tozer, S. W. & Latturmer, S. E. (2008). *Chem. Mater.* **20**, 5675–5681.

- Nesper, R. (1990). *Prog. Solid State Chem.* **20**, 1–45.
- Park, S.-M., Kim, S.-J. & Kanatzidis, M. G. (2003). *J. Solid State Chem.* **175**, 310–315.
- Pfuner, F., Degiorgi, L., Ott, H.-R., Bianchi, A. & Fisk, Z. (2008). *Phys. Rev. B*, **77**, 024417.
- Shannon, R. D. (1976). *Acta Cryst.* **A32**, 751–767.
- Sheldrick, G. M. (2003). *SADABS*. University of Göttingen, Germany.
- Sheldrick, G. M. (2008). *Acta Cryst.* **A64**, 112–122.
- Somer, M., Carrillo-Cabrera, W., Peters, K. & von Schnering, H. G. (1998). *Z. Kristallogr.* **213**, 4.
- Xia, S. Q. & Bobev, S. (2007). *J. Am. Chem. Soc.* **129**, 10011–10018.
- Xia, S. Q. & Bobev, S. (2008). *Inorg. Chem.* **47**, 1919–1921.